

1 $\bar{\text{Ov}}$ Sim: a Simulation of the Population Dynamics of 2 Mammalian Ovarian Follicles

3
4 Joshua Johnson^{1*}, Xin Chen^{1,2}, Xiao Xu¹, John W. Emerson³,

5 1 - Yale School of Medicine, Department of Obstetrics, Gynecology, & Reproductive Sciences, 333
6 Cedar Street, Tompkins 2-203, New Haven, CT, 06520-8063, USA.

7 2 - Center of Reproductive Medicine, Department of Gynecology and Obstetrics, Nanfang Hospital,
8 Southern Medical University, Guangzhou 510515, China.

9 3 - Department of Statistics, Yale University, 24 Hillhouse Avenue, Room B06, New Haven, CT, 06520,
10 USA.

11 * Email address for correspondence: josh.johnson@yale.edu

12 Abstract

13 No two ovaries are alike, and indeed, the same ovary can change its architecture from day to day. This is
14 because ovarian follicles are present in different numbers, positions, and states of maturation throughout
15 reproductive life. All possible developmental states of follicles can be represented at any time, along
16 with follicles that have committed to death (termed follicle atresia). Static histological and whole-mount
17 imaging approaches allow snapshots of what is occurring within ovaries, but our views of dynamic follicle
18 growth and death have been limited to these tools. We present a simple Markov chain model of the
19 complex mouse ovary, called “ $\bar{\text{Ov}}$ Sim”. In the model, follicles can exist in one of four Markov states,
20 Hold (growth arrest), Growth Activate, Grow, and Die. The probability that individual primordial
21 follicles can growth activate daily, the fraction of granulosa cells that survive as follicles grow, and the
22 probability that individual follicles can commit to atresia daily are user definable parameters. When the
23 probability of daily growth activation is near 0.005, granulosa cell survival is 0.88, and the probability of
24 atresia for all follicles is near 0.1, $\bar{\text{Ov}}$ Sim simulates the growth and fate of each of the approximately 3000
25 postpubertal mouse ovarian follicles in a fashion that closely matches biological measurements. $\bar{\text{Ov}}$ Sim
26 thus offers a starting platform to simulate mammalian ovaries and to explore factors that might impact
27 follicle development and global organ function.

Author Summary

ÖvSim is a computer simulation of the dynamic growth of mouse ovarian follicles. The program is offered as the beginning of a research and teaching platform to model asynchronous follicle growth and survival or death.

Introduction

A central goal in reproductive biology and medicine is determining mechanisms that control the fates of mammalian ovarian follicles. This is because follicle growth and survival control the availability of the mature eggs used for conception. Follicles also produce endocrine hormones that are key not only for reproduction, but that support health and quality of life. An ovarian follicle consists of a single oocyte and associated somatic cells. After a period of growth arrest in a ‘primordial’ follicle state, growth activation can occur *via* upregulation of mTOR/Akt signaling (1, 4, 12, 23, 31). Somatic granulosa cells begin to proliferate around the oocyte, which itself grows in size and later resumes and completes meiosis (3, 29). Few follicles survive to the final ovulatory stage where they can release a mature egg; the majority of follicles die within the ovary in a process called atresia (11, 14, 39). Because follicles are present in the thousands in reproductive-age mice and humans, and their growth, development and death occur in an asynchronous, stochastic fashion, it can be difficult to conceptualize the ovary’s function(s) as an endocrine organ and its regular production of eggs.

The most common approaches used to account for the developmental states and survival (or death) of follicles is the preparation of static histological sections. These are referred to as histomorphometric approaches (11, 18, 38). Histological sections allow a very detailed micron-scale appreciation for all of the cell types and structures in and around follicles. More recently, whole-mount fluorescence analysis has been used to great effect, providing a finely-grained accounting of the numbers and sizes of follicle-enclosed oocytes (9, 22). Future modifications of this latter approach may eventually allow for computer-assisted analysis of the disposition of the somatic cells of follicles as well. Experience with the laborious process of histomorphometric follicle counting and analysis led us to question whether an *in silico* approach of simulation and analysis was possible.

Tools for the simulation and visualization of dynamic follicle development within the mammalian ovary have not been available. We hypothesized that establishing a simple set of rules for i) follicle

56 growth activation, ii) granulosa cell proliferation, iii) granulosa cell death, and iv) individual follicle
 57 survival could provide the necessary starting points for a rudimentary simulation of stochastic follicle
 58 behavior over time. Consideration of these rules led us to a Markov chain approach, and to our specifying
 59 the Markov states that follicle can exist within. We reasoned that follicles can exist as growth arrested
 60 primordial follicles (the “Hold” state), as newly growth-activated follicles (the “Activate” state), growing
 61 follicles (the “Grow” state), and follicles that have committed to die *via* atresia (the “Die” state). Markov
 62 state transition models have been applied as powerful tools in the health and medical literature (e.g., in
 63 disease models) (15, 20, 21, 28, 36), and initial modeling of follicles in this way proved fruitful.

64 We then produced a function in the R language (30), providing the ability to conduct simulations
 65 of follicle population development that vary based on the user-specified probabilities assigned to the
 66 follicle states. To our surprise, the simple probability model can produce remarkably accurate represen-
 67 tations of follicle population dynamics, closely matching the biologically observed number of surviving
 68 follicles (and thus an estimate of ovulated eggs) over time. Although this does not prove that the ap-
 69 parently complex process of follicle population dynamics is simple, the results show that a relatively
 70 simple probability-dependent process is consistent with and could help us better understand the process
 71 of follicle development in nature.

72 Materials and Methods

73 `ÖvSim` R code and accompanying documentation is available on GitHub ([https://github.com/](https://github.com/johnsonlab/OvSim)
 74 `johnsonlab/OvSim`) and has been released using the MIT License ([http://opensource.org/](http://opensource.org/licenses/MIT)
 75 `licenses/MIT`; see Supporting Information). `ÖvSim` was designed using known biological paramete-
 76 ters of ovarian follicles while allowing users to modify some of these parameters. Once the script is
 77 activated, a numerical matrix is populated with values corresponding to the starting number of gran-
 78 ulosa cells in individual simulated follicles. The matrix is initially populated with primordial follicles,
 79 randomly-generated such that they can contain one, two, or three pregranulosa cells (Telfer *et al.* (37);
 80 see also “puberty” option below). A simplified example of the Markov matrix operations that simulate
 81 follicle growth is seen as follows (1), where three follicles, *A*, *B*, and *C* are represented by vertical matrix
 82 entries populated by one, two, or three “granulosa cells.”

$$\begin{array}{ccccc}
& A & B & C & \\
Start = & 1 & \underline{\mathbf{3}} & \underline{\mathbf{1}} & \\
\rightarrow & & & & \\
Step1 = & 1 & \underline{\mathbf{3}} & \underline{\mathbf{1}} & \\
& 1 & \underline{\mathbf{6}} & \underline{\mathbf{2}} & \\
\rightarrow & & & & \\
Step2 = & 1 & \underline{\mathbf{3}} & \underline{\mathbf{1}} & \dots \\
& 1 & \underline{\mathbf{6}} & \underline{\mathbf{2}} & \\
& 1 & \underline{\mathbf{10}^*} & \underline{\mathbf{0}^{**}} &
\end{array} \quad (1)$$

83

84 Here, *Start* represents an initial state of three “follicles,” one of which will remain growth-arrested and
85 maintain its number of pregranulosa cells (*A*), and two of which will growth activate in *Step1*, (*B* and
86 *C*, indicated by bold, underlined numbers). The two growing follicles double in population at each step,
87 minus a modeled number of granulosa cells that die. In *Step2*, follicle *B* is shown (*) to contain less than
88 double the number of granulosa cells in the previous step due to granulosa cell death. Follicle *C* grew
89 in *Step1*, but commits to atresia in *Step2*, and its granulosa cell number is set to zero (**, see details
90 below).

91 In $\bar{O}vSim$, the starting number of follicles in the ovary (*NF*), the number of days of time (*ND*) to run
92 the simulation, and the length of the ovulatory cycle (*cyclength*) can all be specified. We set the number
93 of mouse ovarian follicles to 3000, including 2250 primordial follicles (after Tilly (38) and Johnson *et al.*
94 (17)) for most of our studies. Ovulatory cycle length for mice was set at 4, 4.5, or 5 days. The script
95 then continues to loop with “daily” probability calculations and operations upon each follicle entry in
96 the matrix. A flow chart of the operations upon each matrix entry is shown in Figure 1. Simulations run
97 for 420 days by default (14 months), corresponding approximately the fertile lifespan of C57Bl/6 mice
98 fed *ad libitum* (34).

99 Parameters related to follicle growth can be specified as follows. *phold* is the probability that a
100 primordial follicle stays growth arrested each day. Individual primordial follicles either stay arrested and
101 therefore maintain their cell number of 1, 2, or 3, or, growth activate. Growth activation releases that
102 follicle represented in the matrix to a state of exponential granulosa cell growth with a daily doubling
103 time. Granulosa cell number is then controlled by the probability that individual cells within a growing
104 follicle survive (*pcelllive*). Our estimates using histological sections detect a background of pyknotic
105 granulosa cells between 15 and 20% within follicles thought to be intact. Thus (*pcelllive*) is modeled as

106 independent Bernoulli random variable within that range with 0.8 as the default value.

107 To control the fraction of follicles that commit to atresia, a conditional probability, *cond.pdub* is
 108 executed upon each matrix entry each day. As mentioned, the follicle's matrix entry can double (minus
 109 the cell death induced by *pcelllive*, above) with probability *cond.pdub*. Alternatively, the follicle can "die"
 110 via atresia with the probability $1 - \text{cond.pdub}$. A follicle's death is simulated by its matrix entry being
 111 set to zero.

112 The parameter *ejectnum* (50,000 by default) reflects the number of granulosa cells required for a follicle
 113 to be categorized as a fully mature preovulatory follicle. Critically, the simulation as designed here does
 114 not control the final stage(s) of follicle development that ensure that ovulation occurs on only one day
 115 per cycle. For now, we are modeling growth patterns that can give rise to approximately ovulatory sized
 116 follicles within an entire single ovulatory cycle (4 - 5 days in the mouse). Using Pedersen and Peters (29)
 117 as a guide, we set the threshold for survival to ovulation to 50,000 but experimented with thresholds as
 118 large as 500,000 granulosa cells.

119 *****

120 **Line 106. Okay, here I realize I may have been misled above. Not sure what the 2250**
 121 **referred to. But looking at the code I think we currently allow the range go as high as**
 122 **65,000 (2^{16}) so maybe we need to change the code? Perhaps we should only go as high as**
 123 **2^{15} for this initialization? Obviously we have IGP, but I'm not sure of what you mean by**
 124 **"range granulosa cells..." at the bottom of page 4.**

125 JJ: As I understand it, the "IGP" pool of follicles have a range of granulosa cells at start - and I thought
 126 this could only be as high as 20,000. If it can be as high as 65,000, those follicles would be maximum
 127 size at the beginning and yes, it would need to be lowered to $j = \text{half the } 50,000 \text{ threshold}$. Hope we're
 128 talking about the same thing.

129 *****

130 We also added the ability to optionally begin the simulation placing the ovary in a peripubertal state,
 131 where several hundred follicles have already reached the preantral stage of growth awaiting puberty.
 132 The option "puberty," when set to TRUE, populates a user-specified number of matrix entries (variable
 133 IGP for initial growing pool) with granulosa cell numbers that range from growth-activated to 20,000,
 134 an estimate of the number of granulosa cells in peripubertal preantral follicles. The number of growing
 135 follicles and the range of granulosa cells in this prepubertal growing pool can also be user defined.

Results

Using $\bar{\text{OvSim}}$ to Simulate the Mouse Ovary

To model the development of mouse ovarian follicles over a normal reproductive lifespan, the parameters in the *follicle* function are initialized with “default” values shown in the following function declaration:

```
follicle <- function(NF = 3000,
                     ND = 420,
                     IGP = 300,
                     phold = 0.995,
                     cond.pdub = 0.9,
                     pcelllive = 0.8,
                     cyclength = 4,
                     ejectnum = 50000,
                     puberty = TRUE,
                     verbose = TRUE,
                     pdfname = NA)
{
```

Here, 3000 total follicles are present at the start, 2300 of which are primordial (1-3 granulosa cells), and 700 are small growing follicles randomly modeled to contain up to 20,000 granulosa cells. The estrus cycle length is 4 days. A Markov chain state transition matrix for the probabilities of our four states (Hold, Activate, Grow, and Die) is shown as follows in (2):

$$P = \begin{bmatrix} 0.995 & 0.005 & 0 & 0 \\ 0 & 0 & 0.9 & 0.1 \\ 0 & 0 & 0.9 & 0.1 \\ 0 & 0 & 0 & 1 \end{bmatrix} \quad (2)$$

Figure 1 is a Markov state transition diagram of the probabilities in this matrix. Representative plots of $\bar{\text{OvSim}}$ output when an approximately 6-week-old mouse ovary is simulated using these default settings are shown in Figure 2. The output includes the number of total atretic follicles for this simulated run (2280; along with the corresponding percentage of follicles that die over the run, 65.14%). The total

number of eggs that ovulated was 380, and the total number of intact follicles that remained at the end of the run (primordial or growing) was 340.

Panel 2A shows the trend of decline of the primordial pool over time after execution of the simulation 1000 times. The plot depicts the 1st and 99th percentiles of simulation data (A, gray hatched area). Individual data points for actual counts of C57Bl/6 mouse follicles in histological sections at 6 weeks, 8 months, and 12 months are overlaid with simulated data (circles). Panel 2B is a plot of the growth and death of individual follicles that die within the 420 days of simulated time. Granulosa cell number is represented by the dashed lines, and the time (and follicle “size”) of death is indicated by the letter “D.” Last, Panel 2C is a histogram plot of the distribution of follicles that survive to ovulatory size, grouped in 4 day increments equivalent to the modeled estrus (e.g., ovulatory) cycle length. The number of eggs available for ovulation each cycle are therefore depicted. $\bar{\text{OvSim}}$ also provides for CSV-formatted data associated with these plots, useful for finer analyses of ovulatory follicle number.

For this run, a maximum of 22 ovulatory size follicles were available in the fourth estrus cycle (18 days after simulation start). An average of 4.1 and a median of 3 ovulatory size follicles were produced per estrus cycle.

Application of $\bar{\text{OvSim}}$ to human follicle dynamics

Simulation parameters can also be set to conditions mimicking the human ovary, ovulatory cycle length, and approximate reproductive lifespan. For a preliminary human simulation, we set an appropriate number of human primordial follicles at (50,000), the menstrual cycle length to 30 days, and simulated 35 years (unique variable Y) of reproductive life. We specified that approximately 1 in 10,000 primordial follicles growth activated per day (phold=0.9999) but kept the follicle survival rate (cond.pdub) and the probability that individual granulosa cells (pcelllive) survive the same as in the mouse simulations (0.88 and 0.75, respectively). For the larger human periovulatory follicle, we set the number of granulosa cells at 500,000. A summary of these parameters as entered follows here.

```
human <- function(NF = 50000,
                  Y = 35,
                  ND = 365*Y,
                  IGP = 0,
                  phold = 0.9999,
                  cond.pdub = 0.88,
```

```

191         pcelllive = 0.75,
192         ejectnum = 500000,
193         cyclength = 30,
194         puberty = FALSE,
195         verbose = TRUE,
196         pdfname = NA)
197     {

```

198 Representative output from these settings showed follicles that die or survive to ovulatory size in
199 numbers that were reminiscent of human biological outcomes. The total number of follicles that survived
200 to periovulatory size (contain 500,000 granulosa cells) was 605, and the total number of atretic follicles
201 over time was 35403. This meant that 1.4 follicles survived to periovulatory size per month over the
202 length of the simulation.

203 Discussion

204 The $\bar{\text{OvSim}}$ function simulates ovarian follicle growth using user-definable parameters; when set appropri-
205 ately, simulations produce results that closely match numbers seen over reproductive life *in vivo*. Follicles
206 that growth activate, die, and reach ovulatory size match the numbers seen *in vivo* over time. We em-
207 phasize that this is a very simple simulation that does not take into account known features of biological
208 follicle development. For example, in the mouse and human ovary, paracrine signaling interactions be-
209 tween follicles impact follicle growth activation (6) and perhaps follicle survival (24, 43). Anti-Müllerian
210 hormone (AMH) produced by growing follicles has been shown to inhibit the growth-activation of pri-
211 mordial follicles (6, 7, 8). If AMH action were simulated in $\bar{\text{OvSim}}$, such that follicle growth activation
212 accelerated as the number of growing follicles depleted, it is likely that the curve of simulated primordial
213 follicle number in Figure 2A would more precisely match the histomorphometric follicle numbers counted
214 at 1 year of age. We will work to include finer details of follicle biology in this simulation, including the
215 effects of modeled paracrine and endocrine signaling. What is clear, however is that constant growth
216 activation and death rates in our simple model can result in biologically-relevant numbers of follicles that
217 survive to the ovulatory stage or die.

218 $\bar{\text{OvSim}}$ trials show that just a few control parameters can give rise to patterns of asynchronous follicle
219 growth that appear complex. For this initial simulation, the control parameters do not include any

simulation of interaction(s) between follicles. Follicle development within mammalian ovaries may in some ways fit the criteria for the phenomenon called emergent behavior (5, 32). Emergent behavior or emergent property(ies) can appear when a number of simple entities (here, follicles) operate in an environment and form more complex behaviors as a collective (the ovary). Another definition of emergent behavior is any behavior of a system that is not a property of any of the components of that system (5). The mouse (and human) ovary can be modeled as a “system of systems” where overall organ behavior can arise from, but is not necessarily a property of, individual follicles. It is also important to consider how synchronization occurs such that those follicles that survive to reach ovulatory size ovulate together on a single day.

The problem of synchronous follicle *availability* for ovulation can be solved by simple rules, but not the more precise follicle *synchronization* such that all periovulatory follicles ovulate on a single day. Selection for ovulation is solved by an additional layer of complexity, the hormonal ovulatory cycle. Ovulation and the final stages of meiotic maturation occur after the LH surge on a single day of the ovulatory cycle, favoring the production of mature eggs on the day of ovulation as well. The hormonal ovulatory cycle can be considered as a “binning” or “winnowing” mechanism, acting upon and selecting follicles of appropriate size to ensure that an appropriate number are ovulated only one day per cycle. The word winnowing can imply the removal of undesirable elements, as in the potential removal of poorer quality oocytes, but whether selection for high quality eggs does occur *in vivo* is unclear (16, 40, 41).

Ensuring that the number of eggs ovulated is tightly regulated in female mammals can be a matter of life or death. Ovulating too few eggs could compromise the survival of a species if too few offspring were produced over time. Ovulating too many eggs can also compromise the survival of a species. Multiple gestation in humans is well known to be a significant risk factor for maternal and offspring loss of life (2, 33, 42). Evolving mechanisms to ensure that the correct number of eggs are produced within an organism’s overall reproductive strategy would therefore have been favored. It is striking that simple regulatory mechanisms (e.g., constant growth activation and atresia rates) can solve much of the problem of the periodic production of ‘safe’ numbers of eggs. Adding a level of ovulatory cyclicity to a future version of ŌvSim will allow the control of ovulation timing to be simulated, and may provide clues about the evolution of the ovulatory cycle itself.

Knowing that simple rules can control the number of follicles at different stages of development and death in a fashion that mimics ovarian biology opens the question of how close such simulations come to reality. ‘Wet lab’ experiments can be designed to test whether such simple rules underlie ovarian

function *in vivo*, and if so, what mechanisms enforce those rules. What mechanisms could control a fixed approximate 1% growth activation rate and 10% overall atresia rate? How could seemingly equivalent primordial follicles growth activate at such a constant rate without activating too quickly or slowly, ensuring that the total duration of ovarian function is appropriate for the reproductive strategy of the female? How can the rate of follicle atresia similarly remain so constant? Premature cessation of ovarian function could result if the rate of either growth activation or atresia were increased (see Silber (35) for a review). $\bar{\text{OvSim}}$ can also be modified to model questions that are even more theoretical, such as the impact of ovotoxic agents (e.g., chemotherapeutic or radiological intervention(s)) upon the duration of ovarian function, or, the impact of the additional of new follicles postnatally as suggested by studies that support postnatal oogenesis.

The current prevailing consensus in the field is that oogenesis and folliculogenesis ceases before or around birth in most mammals. However, since the first paper calling this into question (17), evidence continues to build that postnatal follicle development can occur *via* the action of female germline stem cells (FGSC) (13, 19, 26, 27, 44, 45, 46, 47, 48, 49, 50, 51). FGSC are currently being used as a source of mitochondria (see Woods and Tilly (46) for a review) for delivery to oocyte cytoplasm in attempts to improve egg quality and pregnancy rates in the clinic (10, 25). It is a relatively trivial matter to modify the $\bar{\text{OvSim}}$ *follicles* function so that new follicles are added at a desired rate and the impact upon the trajectory of follicle loss over time can be estimated. We will continue to develop flexible tools like $\bar{\text{OvSim}}$ to address these exciting questions, and hope that other groups will modify the package and build on this approach.

Supporting Information

$\bar{\text{OvSim}}$ Package Installation

All package and supporting files are available on GitHub (<https://github.com/REPOSITORY>) and has been released using the MIT License (<http://opensource.org/licenses/MIT>). $\bar{\text{OvSim}}$ can be installed in an R Environment by following the instructions in the file README.md. Alternatively, the single text file `ovsim.R` can be executed within R after optional alteration of individual parameters.

277 **ÖvSim Package License**

278 ÖvSim is available under the conditions of The MIT License (MIT)

279 © 2015 Joshua Johnson and John W. Emerson

280 Permission is hereby granted, free of charge, to any person obtaining a copy of this software and associated
281 documentation files (the "Software"), to deal in the Software without restriction, including without
282 limitation the rights to use, copy, modify, merge, publish, distribute, sublicense, and/or sell copies of the
283 Software, and to permit persons to whom the Software is furnished to do so, subject to the following
284 conditions:

285 The above copyright notice and this permission notice shall be included in all copies or substantial
286 portions of the Software.

287 THE SOFTWARE IS PROVIDED "AS IS", WITHOUT WARRANTY OF ANY KIND, EXPRESS OR
288 IMPLIED, INCLUDING BUT NOT LIMITED TO THE WARRANTIES OF MERCHANTABILITY,
289 FITNESS FOR A PARTICULAR PURPOSE AND NONINFRINGEMENT. IN NO EVENT SHALL
290 THE AUTHORS OR COPYRIGHT HOLDERS BE LIABLE FOR ANY CLAIM, DAMAGES OR
291 OTHER LIABILITY, WHETHER IN AN ACTION OF CONTRACT, TORT OR OTHERWISE, ARISING
292 FROM, OUT OF OR IN CONNECTION WITH THE SOFTWARE OR THE USE OR OTHER
293 DEALINGS IN THE SOFTWARE.

294 **Funding**

295 These studies were supported by a Milstein Medical Asian American Partnership Foundation Fellowship
296 Award in Reproductive Medicine (X.C.) and The Albert McKern Fund for Perinatal Research (J.J.).

297 **Acknowledgements**

298 Drs. Giovanni Cottichio and Taiwo Togun are acknowledged for comments upon the manuscript prior to
299 submission.

Table 1. $\bar{\text{OvSim}}$ User-Specified Parameters

Parameter Name	Description
NF	Number of follicles to be simulated.
ND	Number of days for simulation to run.
IGP	Initial growing pool of follicles (when puberty is set to TRUE).
phold	Probability that a follicle stays growth arrested or begins to grow.
cond.pdub	Conditional probability that a follicle either continues to grow or dies.
pcelllive	Probability that granulosa cells live, modeled as independent Bernoulli random variable.
cyclength	Length in days of simulated female reproductive cycle.
ejectnum	Threshold number of granulosa cells for a follicle to be categorized as pre-ovulatory size.
puberty	When TRUE, sets the number of follicles specified in IGP as growing.
verbose	When TRUE, verbose output of simulation is provided.
pdfname	Desired name of .pdf simulation output.

References

1. Adhikari, D., Gorre, N., Risal, S., Zhao, Z., Zhang, H., Shen, Y., and Liu, K. (2012). The safe use of a PTEN inhibitor for the activation of dormant mouse primordial follicles and generation of fertilizable eggs. *PLoS ONE*, **7**(6), e39034.
2. Ananth, C. V., Joseph Ks, K. s., and Smulian, J. C. (2004). Trends in twin neonatal mortality rates in the United States, 1989 through 1999: influence of birth registration and obstetric intervention. *Am. J. Obstet. Gynecol.*, **190**(5), 1313–1321.
3. Anderson, L. D. and Hirshfield, A. N. (1992). An overview of follicular development in the ovary: from embryo to the fertilized ovum in vitro. *Md Med J*, **41**(7), 614–620.
4. Cheng, Y., Kim, J., Li, X. X., and Hsueh, A. J. (2015). Promotion of ovarian follicle growth following mTOR activation: synergistic effects of AKT stimulators. *PLoS ONE*, **10**(2), e0117769.
5. Cohen, I. R. and Harel, D. (2007). Explaining a complex living system: dynamics, multi-scaling and emergence. *J R Soc Interface*, **4**(13), 175–182.
6. Durlinger, A. L., Kramer, P., Karels, B., de Jong, F. H., Uilenbroek, J. T., Grootegoed, J. A., and Themmen, A. P. (1999). Control of primordial follicle recruitment by anti-Müllerian hormone in the mouse ovary. *Endocrinology*, **140**(12), 5789–5796.
7. Durlinger, A. L., Gruijters, M. J., Kramer, P., Karels, B., Kumar, T. R., Matzuk, M. M., Rose, U. M., de Jong, F. H., Uilenbroek, J. T., Grootegoed, J. A., and Themmen, A. P. (2001). Anti-Müllerian hormone attenuates the effects of FSH on follicle development in the mouse ovary. *Endocrinology*, **142**(11), 4891–4899.
8. Durlinger, A. L., Gruijters, M. J., Kramer, P., Karels, B., Ingraham, H. A., Nachtigal, M. W., Uilenbroek, J. T., Grootegoed, J. A., and Themmen, A. P. (2002). Anti-Müllerian hormone inhibits initiation of primordial follicle growth in the mouse ovary. *Endocrinology*, **143**(3), 1076–1084.
9. Faire, M., Skillern, A., Arora, R., Nguyen, D. H., Wang, J., Chamberlain, C., German, M. S., Fung, J. C., and Laird, D. J. (2015). Follicle dynamics and global organization in the intact mouse ovary. *Dev. Biol.*, **403**(1), 69–79.

- 326 10. Fakih, M., El Shmoury, M., Szeptycki, J., de la Cruz, D., Lux, C., Verjee, S., Burgess, C., and
 327 Casper, R. (2015). The AUGMENTSM Treatment: Physician Reported Outcomes of the Initial
 328 Global Patient Experience. *J.F.I.V. Reprod. Med. Genet.*, **3**, 154.
- 329 11. Hirshfield, A. N. (1991). Development of follicles in the mammalian ovary. *Int. Rev. Cytol.*, **124**,
 330 43–101.
- 331 12. Hsueh, A. J., Kawamura, K., Cheng, Y., and Fauser, B. C. (2015). Intraovarian control of early
 332 folliculogenesis. *Endocr. Rev.*, **36**(1), 1–24.
- 333 13. Imudia, A. N., Wang, N., Tanaka, Y., White, Y. A., Woods, D. C., and Tilly, J. L. (2013).
 334 Comparative gene expression profiling of adult mouse ovary-derived oogonial stem cells supports a
 335 distinct cellular identity. *Fertil. Steril.*, **100**(5), 1451–1458.
- 336 14. Inoue, S., Watanabe, H., Saito, H., Hiroi, M., and Tonosaki, A. (2000). Elimination of atretic
 337 follicles from the mouse ovary: a TEM and immunohistochemical study in mice. *J. Anat.*, **196** (Pt
 338 1), 103–110.
- 339 15. Jit, M. and Brisson, M. (2011). Modelling the epidemiology of infectious diseases for decision
 340 analysis: a primer. *Pharmacoeconomics*, **29**(5), 371–386.
- 341 16. Johnson, J. and Keefe, D. L. (2013). Ovarian aging: breaking up is hard to fix. *Sci Transl Med*,
 342 **5**(172), 172fs5.
- 343 17. Johnson, J., Canning, J., Kaneko, T., Pru, J. K., and Tilly, J. L. (2004). Germline stem cells and
 344 follicular renewal in the postnatal mammalian ovary. *Nature*, **428**(6979), 145–150.
- 345 18. Kerr, J. B., Duckett, R., Myers, M., Britt, K. L., Mladenovska, T., and Findlay, J. K. (2006).
 346 Quantification of healthy follicles in the neonatal and adult mouse ovary: evidence for maintenance
 347 of primordial follicle supply. *Reproduction*, **132**(1), 95–109.
- 348 19. Khosravi-Farsani, S., Amidi, F., Habibi Roudkenar, M., and Sobhani, A. (2015). Isolation and
 349 enrichment of mouse female germ line stem cells. *Cell J*, **16**(4), 406–415.
- 350 20. Kirsch, F. (2015). A systematic review of quality and cost-effectiveness derived from Markov models
 351 evaluating smoking cessation interventions in patients with chronic obstructive pulmonary disease.
 352 *Expert Rev Pharmacoecon Outcomes Res*, **15**(2), 301–316.

- 353 21. Lampert, A. and Korngreen, A. (2014). Markov modeling of ion channels: implications for under-
354 standing disease. *Prog Mol Biol Transl Sci*, **123**, 1–21.
- 355 22. Malki, S., Tharp, M. E., and Bortvin, A. (2015). A Whole-Mount Approach for Accurate Quanti-
356 tative and Spatial Assessment of Fetal Oocyte Dynamics in Mice. *Biol. Reprod.*, **93**(5), 113.
- 357 23. McLaughlin, M., Kinnell, H. L., Anderson, R. A., and Telfer, E. E. (2014). Inhibition of phosphatase
358 and tensin homologue (PTEN) in human ovary in vitro results in increased activation of primordial
359 follicles but compromises development of growing follicles. *Mol. Hum. Reprod.*, **20**(8), 736–744.
- 360 24. Moley, K. H. and Schreiber, J. R. (1995). Ovarian follicular growth, ovulation and atresia. En-
361 docrine, paracrine and autocrine regulation. *Adv. Exp. Med. Biol.*, **377**, 103–119.
- 362 25. Oktay, K., Baltaci, V., Sonmezer, M., Turan, V., Unsal, E., Baltaci, A., Aktuna, S., and Moy, F.
363 (2015). Oogonial Precursor Cell-Derived Autologous Mitochondria Injection to Improve Outcomes
364 in Women With Multiple IVF Failures Due to Low Oocyte Quality: A Clinical Translation. *Reprod*
365 *Sci*, **22**(12), 1612–1617.
- 366 26. Pacchiarotti, J., Maki, C., Ramos, T., Marh, J., Howerton, K., Wong, J., Pham, J., Anorve, S.,
367 Chow, Y. C., and Izadyar, F. (2010). Differentiation potential of germ line stem cells derived from
368 the postnatal mouse ovary. *Differentiation*, **79**(3), 159–170.
- 369 27. Park, E. S., Woods, D. C., and Tilly, J. L. (2013). Bone morphogenetic protein 4 promotes
370 mammalian oogonial stem cell differentiation via Smad1/5/8 signaling. *Fertil. Steril.*, **100**(5), 1468–
371 1475.
- 372 28. Parker, W. H., Broder, M. S., Liu, Z., Shoupe, D., Farquhar, C., and Berek, J. S. (2007). Ovarian
373 conservation at the time of hysterectomy for benign disease. *Clin Obstet Gynecol*, **50**(2), 354–361.
- 374 29. Pedersen, T. and Peters, H. (1968). Proposal for a classification of oocytes and follicles in the
375 mouse ovary. *J. Reprod. Fertil.*, **17**(3), 555–557.
- 376 30. R Development Core Team (2008). R: A language and environment for statistical computing. ISBN
377 3-900051-07-0.
- 378 31. Reddy, P., Liu, L., Adhikari, D., Jagarlamudi, K., Rajareddy, S., Shen, Y., Du, C., Tang, W.,
379 Hamalainen, T., Peng, S. L., Lan, Z. J., Cooney, A. J., Huhtaniemi, I., and Liu, K. (2008).

- Oocyte-specific deletion of Pten causes premature activation of the primordial follicle pool. *Science*,
319(5863), 611–613.
32. Saunders, P. and Skar, P. (2001). Archetypes, complexes and self-organization. *J Anal Psychol*,
46(2), 305–323.
33. Sciarra, J. J. and Keith, L. G. (1990). Multiple pregnancy: an international perspective. *Acta
Genet Med Gemellol (Roma)*, **39**(3), 353–360.
34. Selesniemi, K., Lee, H. J., and Tilly, J. L. (2008). Moderate caloric restriction initiated in rodents
during adulthood sustains function of the female reproductive axis into advanced chronological age.
Aging Cell, **7**(5), 622–629.
35. Silber, S. (2015). Unifying theory of adult resting follicle recruitment and fetal oocyte arrest.
Reprod. Biomed. Online, **31**(4), 472–475.
36. Singh, J. A., Cameron, C., Noorbaloochi, S., Cullis, T., Tucker, M., Christensen, R., Ghogomu,
E. T., Coyle, D., Clifford, T., Tugwell, P., and Wells, G. A. (2015). Risk of serious infection in
biological treatment of patients with rheumatoid arthritis: a systematic review and meta-analysis.
Lancet, **386**(9990), 258–265.
37. Telfer, E., Ansell, J. D., Taylor, H., and Gosden, R. G. (1988). The number of clonal precursors of
the follicular epithelium in the mouse ovary. *J. Reprod. Fertil.*, **84**(1), 105–110.
38. Tilly, J. L. (2003). Ovarian follicle counts—not as simple as 1, 2, 3. *Reprod. Biol. Endocrinol.*, **1**,
11.
39. Tilly, J. L., Kowalski, K. I., Johnson, A. L., and Hsueh, A. J. (1991). Involvement of apoptosis in
ovarian follicular atresia and postovulatory regression. *Endocrinology*, **129**, 2799–2801.
40. Titus, S., Li, F., Stobezki, R., Akula, K., Unsal, E., Jeong, K., Dickler, M., Robson, M., Moy, F.,
Goswami, S., and Oktay, K. (2013). Impairment of BRCA1-related DNA double-strand break repair
leads to ovarian aging in mice and humans. *Sci Transl Med*, **5**(172), 172ra21.
41. Titus, S., Stobezki, R., and Oktay, K. (2015). Impaired DNA Repair as a Mechanism for Oocyte
Aging: Is It Epigenetically Determined? *Semin. Reprod. Med.*

- 406 42. Uthman, O. A., Uthman, M. B., and Yahaya, I. (2008). A population-based study of effect of
407 multiple birth on infant mortality in Nigeria. *BMC Pregnancy Childbirth*, **8**, 41.
- 408 43. Webb, R. and Campbell, B. K. (2007). Development of the dominant follicle: mechanisms of
409 selection and maintenance of oocyte quality. *Soc Reprod Fertil Suppl*, **64**, 141–163.
- 410 44. White, Y. A., Woods, D. C., Takai, Y., Ishihara, O., Seki, H., and Tilly, J. L. (2012). Oocyte
411 formation by mitotically active germ cells purified from ovaries of reproductive-age women. *Nat.*
412 *Med.*, **18**(3), 413–421.
- 413 45. Woods, D. C. and Tilly, J. L. (2013). Isolation, characterization and propagation of mitotically
414 active germ cells from adult mouse and human ovaries. *Nat Protoc*, **8**(5), 966–988.
- 415 46. Woods, D. C. and Tilly, J. L. (2015). Autologous Germline Mitochondrial Energy Transfer (AUG-
416 MENT) in Human Assisted Reproduction. *Semin. Reprod. Med.*
- 417 47. Xie, W., Wang, H., and Wu, J. (2014). Similar morphological and molecular signatures shared by
418 female and male germline stem cells. *Sci Rep*, **4**, 5580.
- 419 48. Zhang, Y., Yang, Z., Yang, Y., Wang, S., Shi, L., Xie, W., Sun, K., Zou, K., Wang, L., Xiong, J.,
420 Xiang, J., and Wu, J. (2011). Production of transgenic mice by random recombination of targeted
421 genes in female germline stem cells. *J Mol Cell Biol*, **3**(2), 132–141.
- 422 49. Zhou, L., Wang, L., Kang, J. X., Xie, W., Li, X., Wu, C., Xu, B., and Wu, J. (2014). Production
423 of fat-1 transgenic rats using a post-natal female germline stem cell line. *Mol. Hum. Reprod.*, **20**(3),
424 271–281.
- 425 50. Zou, K., Yuan, Z., Yang, Z., Luo, H., Sun, K., Zhou, L., Xiang, J., Shi, L., Yu, Q., Zhang, Y., Hou,
426 R., and Wu, J. (2009). Production of offspring from a germline stem cell line derived from neonatal
427 ovaries. *Nat. Cell Biol.*, **11**(5), 631–636.
- 428 51. Zou, K., Hou, L., Sun, K., Xie, W., and Wu, J. (2011). Improved efficiency of female germline stem
429 cell purification using fragilis-based magnetic bead sorting. *Stem Cells Dev.*, **20**(12), 2197–2204.

Figure Legends

Figure 1. Markov state transition diagram of mouse ovarian follicle development. This flow chart shows the simplified logic of follicle development, where two decisions are made based on fixed probabilities that are depicted adjacent to arrows. From left to right, the first decision for an individual primordial follicle (numerical matrix entry of 1, 2, or 3 granulosa cells) is whether to remain arrested or to growth activate. Growth activation introduces a daily doubling of cell number. After growth activation, a follicle may either grow or die daily, with a correction factor of cell death applied to granulosa cell number. If a follicle reaches 50,000 cells, it is categorized as an ovulatory follicle.

Figure 2. Example $\bar{\text{OvSim}}$ mouse ovary output. Default plots produced after an $\bar{\text{OvSim}}$ run with “puberty” option set to TRUE. X-axes shown represent total simulated time in days; pubertal animals would be approximately 50 days old at the start of the simulation. The trajectory of decline of the primordial follicle pool for 1000 $\bar{\text{OvSim}}$ runs is plotted as shown in panel **A** where the gray shaded area is the first and 99th percentiles of run output. Circles are actual data from follicle counts of C57Bl/6 mice at 6 weeks, 8 months, and 12 months of age ($n = 4$ ovaries, each from a different animal). In **B**, the growth history of individual follicles that die *via* atresia in a single run is shown by plotting the number of granulosa cells (dashed line) over time, ending with follicle death denoted by the letter “D.” **C** shows the number of follicles that survive to ovulatory size cutoff (50,000 granulosa cells) each ovulatory cycle (here, 4 days), and dashed vertical lines mark months of time within a single simulation run.

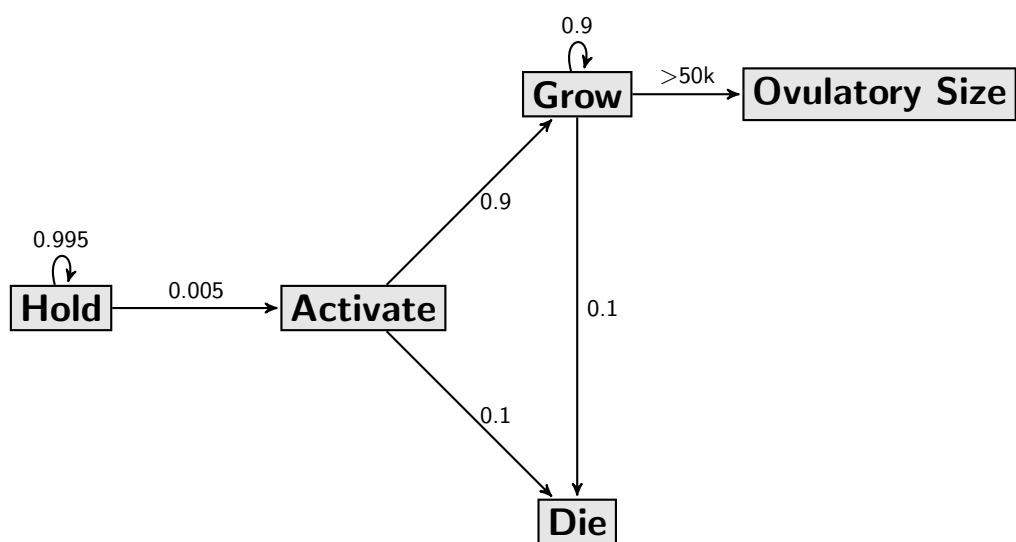


Figure 1. Mouse Ovarian Follicle Markov State Transition Diagram.

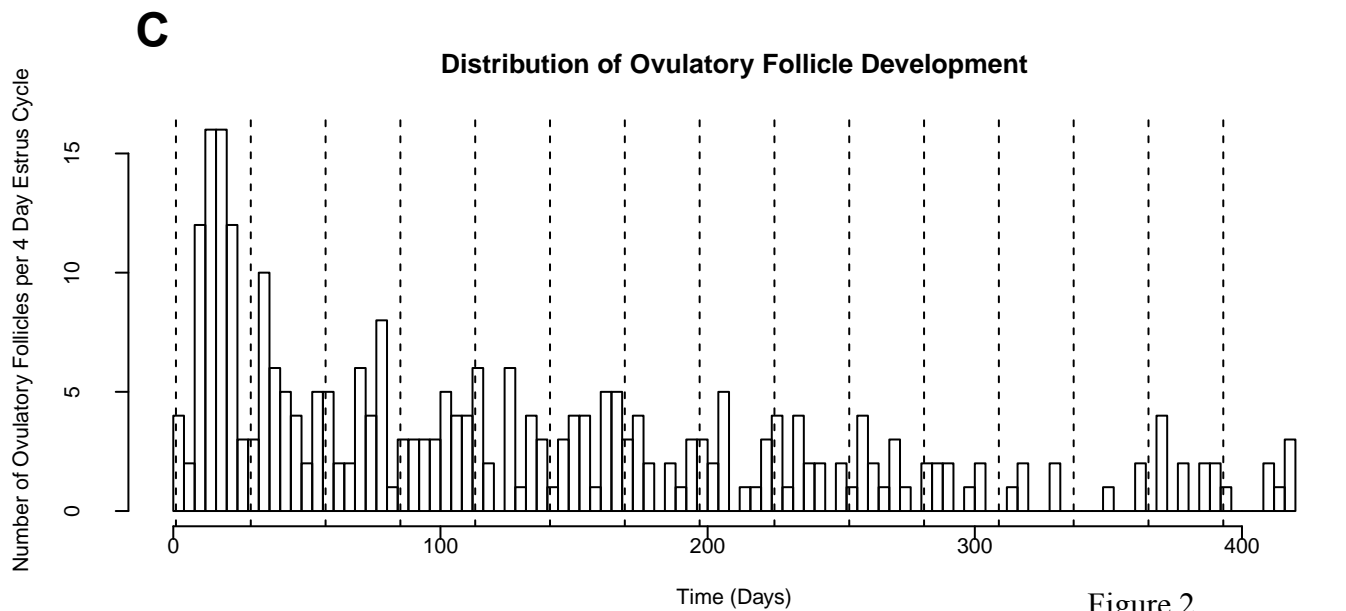
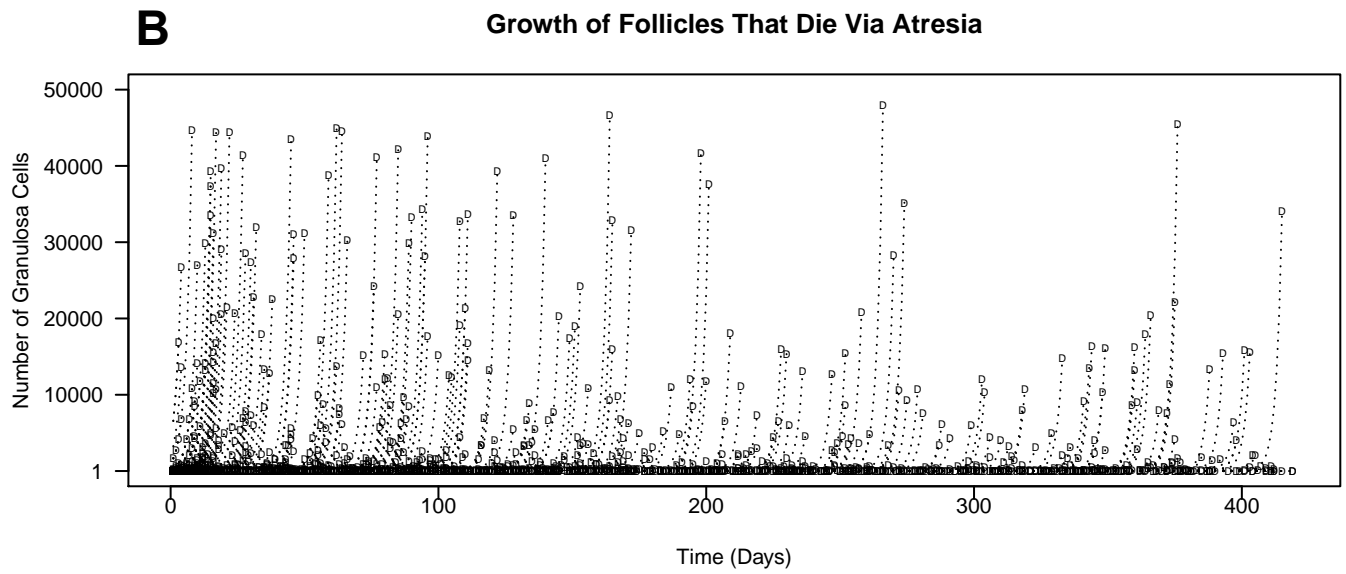
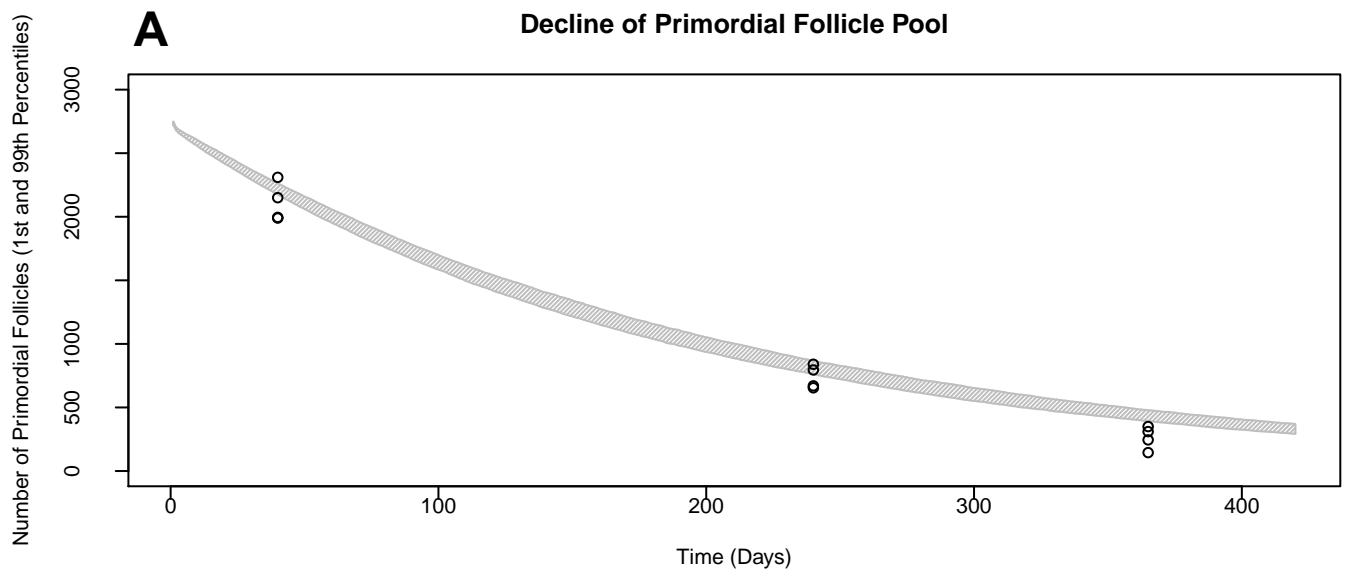


Figure 2.